Subthalamic Nucleus Stimulation Modulates Motor Epileptic Activity in Humans

Liankun Ren, MD, PhD,[1†] Tao Yu, MD,[2†] Di Wang, MD,[1†] Xueyuan Wang, MD, PhD,[2] Duanyu Ni, MD,[2] Guojun Zhang, MD,[2] Fabrice Bartolomei, MD, PhD,[3,4] Yuping Wang, MD, PhD,[1] and Yongjie Li, MD, PhD[2]

Objective: Pharmaco-refractory focal motor epileptic seizures pose a significant challenge. Deep brain stimulation (DBS) is a recently recognized therapeutic option for the treatment of refractory epilepsy. To identify the specific target for focal motor seizures, we evaluate the modulatory effects of the subthalamic nucleus (STN) stimulation because of the critical role of STN in cortico-subcortical motor processing.
Methods: Seven patients with epilepsy with refractory seizures who underwent chronic stereoelectroencephalography (SEEG) monitoring were studied in presurgical evaluation. Seizure onset zone was hypothesized to be partially involved in the motor areas in 6 patients. For each patient, one electrode was temporally implanted into the STN that was ipsilateral to the seizure onset zone. The cortical–subcortical seizure propagation was systemically evaluated. The simultaneously electrophysiological responses over distributed cortical areas to STN stimulation at varied frequencies were quantitatively assessed.
Results: We observed the consistent downstream propagation of seizures from the motor cortex toward the ipsilateral STN and remarkable cortical responses on motor cortex to single-pulse STN stimulation. Furthermore, we showed frequency-dependent upstream modulatory effect of STN stimulation on motor cortex specifically. In contrast to the enhanced effects of low frequency stimulation, high-frequency stimulation of the STN can significantly reduce interictal spikes, high-frequency oscillations over motor cortex disclosing effective connections to the STN.
Interpretation: This result showed that the STN is not only engaged in as a propagation network of focal motor seizures but STN stimulation can profoundly modulate the epileptic activity of motor cortex in humans, suggesting a mechanism-based alternative for patients suffering from refractory focal motor seizures.

ANN NEUROL 2020;00:1–14

Epilepsy is a serious and highly prevalent neurological disease that affects individuals of all ages worldwide. Surgical resection remains a powerful treatment modality for approximately 30% of patients who continue to have seizures despite optimal antiepileptic therapy.[1,2] Nevertheless, pharmaco-refractory focal motor seizures that arise from the motor area, in particular the primary motor cortex are of a significant challenge because of the high risk of an irreversible motor deficit resulting from the removal of this epileptic tissue.[3,4] Therefore, the exploration of alternative therapeutic methods for such patients remains a topic of intensive study. In essence, epilepsy is characterized by excessive electrical discharges due to the imbalance of excitation and inhibition of neural assemblies.

View this article online at wileyonlinelibrary.com. DOI: 10.1002/ana.25776

Received Feb 4, 2020, and in revised form May 7, 2020. Accepted for publication May 7, 2020.

Address correspondence to Drs Liankun Ren, Department of Neurology, Xuanwu Hospital, Capital Medical University, 45 Changchun Street, 100053 Beijing, China. E-mail: rlkbrain2000@yahoo.com; Drs. Tao Yu and Yongjie Li, Department of Functional Neurosurgery, Beijing Institute of Functional Neurosurgery, Xuanwu Hospital, Capital Medical University, Beijing, China. E-mail: yutaoly@sina.com and lyj8828@vip.sina.com
[†]Dr Liankun Ren, Dr Tao Yu, and Dr Di Wang contributed equally to this study.

From the [1]Department of Neurology, Comprehensive Epilepsy Center of Beijing, Beijing Key Laboratory of Neuromodulation, Xuanwu Hospital, Capital Medical University, Beijing, China; [2]Department of Functional Neurosurgery, Beijing Institute of Functional Neurosurgery, Xuanwu Hospital, Capital Medical University, Beijing, China; [3]Department of Clinical Neurophysiology, APHM, Timone Hospital, Marseille, France; and [4]Aix Marseille Univ, INSERM, INS, Institut de Neurosciences des Systèmes, Marseille, France

Additional supporting information can be found in the online version of this article.

© 2020 American Neurological Association

Such aberrant brain activity is speculated to be restored through electrical stimulation. Neuromodulation has emerged as an alternative treatment over a few decades. Based on the real-time detection of ictal discharges patterns and sequentially triggering focal stimulation to abrupt the seizure, closed-loop responsive neurostimulation might be effective for motor cortex seizures.[5,6] Of note, by means of affecting neural networks, deep brain stimulation (DBS) is a recently recognized therapeutic option for the treatment of refractory epilepsy in hope of alleviating seizures without causing the neurological deficits anticipated with resection, particularly for patients who are not eligible for surgical resection.[7,8] To date, various potential brain targets have been stimulated in animal models and clinical investigation,[9,10] and encouraging results have been reported by open-label pilot studies and randomized controlled clinical trials.[8,11,12] Although studies have showed that specific epilepsy patient groups may achieve better outcomes by stimulating certain targets, which suggests the ability of DBS to modify brain dysfunctions might depend on the specific sites in the complex neuronal circuitry involving such functions, the ideal stimulation sites for focal motor seizures has not been determined.[13,14]

Subthalamic nucleus (STN) is an attractive target because of its critical role in cortico-subcortical motor processing.[15,16] Accumulating evidence from experimental data have shown the implications of the basal ganglia structures in focal seizures.[17-19] In a primate model with motor seizures induced by a local injection of penicillin into the motor cortex, Devergnas et al observed that seizures propagated from the motor cortex towards the basal ganglia, in which the external part of the globus pallidus-STN pathway was remarkably affected.[20] They further showed that STN stimulation can improve focal motor seizures by delaying the occurrence of the first seizure and decreasing the number of seizures.[21] Clinically, Benabid and colleagues first indicated a 67% to 80% reduction in seizure frequency in 3 patients with focal epileptic seizures of the central area compared with other regions in the early 2000s.[22,23] Although variability in the outcomes has subsequently been reported in a few patients with heterogeneous epilepsy types,[24-27] patients with motor seizures seemed to benefit more from the treatment of STN-DBS.[10] We recently reported the favorable 5-year outcome of unilateral STN-DBS in one patient with refractory focal myoclonic seizures.[28] To date, STN-DBS as a treatment modality for epilepsy is far from being established. The poor understanding of the mechanisms of action has largely limited the application of STN-DBS for the treatment of epilepsy.

Here, we hypothesize that STN-DBS is a potential therapeutic modality specifically for the treatment of motor seizures. Characterization of the precise role of the STN in human motor seizures and the mechanisms of action of STN-DBS would directly advance both theory and practice. Thus, we assessed the role of the STN in motor seizures and especially the modulatory effects of STN stimulation in 7 patients with epilepsy with refractory focal seizures who underwent stereoelectroencephalography (SEEG) monitoring during presurgical evaluation to precisely delineate the epileptogenic area. For each patient, one SEEG electrode was temporally implanted into the STN that was ipsilateral to the assumed seizure onset zone, which provides a window to: (1) directly observe the cortico-subcortical pathway of motor seizures; and (2) electrically stimulate the STN and simultaneously record the cortical responses.

Subjects and Methods

Subjects

All the patients were enrolled from July 2018 to December 2019 in Xuanwu Hospital, Beijing, China. Twenty-five patients met the criteria: (1) patient with drug-resistant focal epilepsy; (2) patient required intracranial recordings because of insufficient/conflict localizing information, and/or the need to precisely map eloquent cortex; (3) on the clinical grounds only, the plan of implantation of SEEG electrodes include both at least 2 electrodes sampling motor cortex and more than 2 electrodes sampling distributed cortical areas; and (4) patient can cooperate with the paradigm. Among them, 18 patients were excluded because of large encephalomalacia, assumed tumoral lesion, or deformation of the motor cortex, the unavailability of written informed consent, or the patients who were not in charge by this study group. Finally, 7 patients were included. The characteristics of all the patients, including ages, duration of epilepsy, seizure semiology, and other profiles, were presented (Supplementary Table S1). Patients 1, 2, 3, 6, and 7 had frequent, prominent tonic/clonic seizures over one-side of their limbs, which occasionally progressed into bilateral tonic–clonic seizures. Patient 4 suffered from left faciobrachial clustered rhythmic myoclonic jerks. Patient 5 had ictal autonomic symptoms that presented a stereotypic palpitation and difficulty of breathing followed by a frequent impairment of consciousness. Increased signal, thickness of focal gyrus, and/or blurring of the grey-matter junction on magnetic resonance imaging (MRI) were detected on motor areas in Patients 1, 2, and 3, which suggested the features of focal cortical dysplasia. Heterotopia over primary and premotor cortex was identified in Patient 4. Atrophy of insula and ipsilateral putamen was detected in Patient 5. Otherwise, the MRI findings of Patients 6 and 7 were negative.

After an integrated evaluation, seizure onset zone was hypothesized to be partially involved in the motor areas, including the lateral primary motor strip, paracentral lobule, and supplementary motor area, as well as premotor area in Patients 1, 2, 3, 4, 6, and 7 and the insular lobe in Patient 5. The planning of SEEG were scheduled based on clinical grounds.[29] For research purposes, one SEEG electrode targeting the STN that was ipsilateral to the assumed seizure onset zone was designed. One SEEG electrode was designed with the trajectory from the frontal lobe toward the STN to avoid passing the ventricle. Based on the classical anatomic location of the STN, the stereotaxic

coordinates of the STN were refined by direct visualization on the individual T2-weighted MRI. Considering the observations from the treatment of movement disorders that the anatomic position of the active electrode within the sensorimotor part of the STN demonstrates improved clinical outcomes,[30,31] the SEEG electrode was targeted at the dorsolateral part of the STN. The SEEG electrodes were semirigid steel with contacts between 8 and 16 (contact 1 is the lowermost one), 2 mm in length, 0.8 mm in diameter, and 1.5 mm apart. Due to a minimum STN thickness of 5 mm, two contracts of the SEEE electrode can be located into the STN.

This study was approved by the Institutional Review Board Committee in accordance with the ethical standards of the Declaration of Helsinki, and informed consent was obtained from all patients and/or guardians.

Stereotaxic Implantation and Reconstruction of Electrodes

The implantation of SEEG electrodes was performed using an oblique approach. In brief, magnetic resonance venography and magnetic resonance angiography sequences (3.0 T, Siemens) were first conducted before surgery. Each designed trajectory was plotted onto the stereotactic digital cerebral angiogram to avoid major vessel injury in the design of SEEG trajectories. The patient's head was subsequently fixed in a Cosman–Roberts–Wells stereotactic frame (Radionics) with cranium pins while under local anesthesia. A high-resolution computed tomography (CT) scan (Siemens) was acquired, and image fusion was performed with the preoperative volumetric T1 MRI sequences using the NeuroGuide system (STEALTH Framelink; Medtronic). With the patient under general anesthesia, the electrodes were inserted one by one. Finally, the patient underwent a CT scan after electrode implantation to verify the exact location of each electrode and identify postoperative complications.

Using LEAD-DBS software (www.lead-dbs.org),[32] postoperative CT images were linearly co-registered to the preoperative MRI using Statistical Parametrical Mapping 12 (http://www.fil.ion.ucl.ac.uk/spm/) individually. The results of co-registrations were manually adjusted and refined for each patient if needed. Then, the MRI was nonlinearly normalized into the standardized Montreal Neurological Institute (MNI) stereotactic space to reconstruct contact locations using Advanced Normlization Tools (http://stnava.github.io/ANTs/). Thus, the location of each electrode's contacts was registered in the standard MNI stereotactic space. For each electrode, the individual contact coordination on standard MNI space was computed after detecting the starting or deepest point. The bipolar location of local field potentials (LFPs) was then defined as the middle point of the pair of adjacent contacts and the coordination was calculated accordingly.

The shape of the STN in the standard MNI space was defined by the DISTAL atlas.[33] Data visualization was performed using BrainNet viewer (https://www.nitrc.org/projects/bnv/) and Pysurfer (https://pysurfer.github.io).

SEEG Recordings and Electric Stimulation Protocols

SEEG was routinely recorded for 7 to 14 days under video monitoring to capture the habitual clinical seizures after surgery. LFPs were recorded by the Micromed electroencephalography (EEG) data acquisition system sampling at 1,024 Hz and using a 50 Hz notch filter. Simultaneous surface electromyography (EMG) on the bilateral orbicularis oculi muscles was recorded for Patient 4 with brachiofacial myoclonic jerks.

Three different stimulation procedures, including electrically cortical stimulation at 50 Hz, low frequency single pulse stimulation at 1 Hz of the STN, and stepwise increment stimulation of the STN from 10 Hz to 130 Hz at a cycle pattern by an external stimulator (Model 3628 screener; Medtronic), were conducted for distinct purposes.

To map the eloquent cortex, stimulation at 50 Hz (pulse duration 0.3 ms, biphasic rectangular stimuli of alternating polarity) that lasted for 5 seconds was applied to 2 serial adjacent contacts on the cortex through the electrodes. The intensity was gradually increased, ranging from 0.5 to 6 mA, until a clinical effect was produced or after discharges were observed. The patients were instructed to sit in bed rest during the electric cortical stimulation procedure and report any symptoms or clinical changes during the period.

To probe the effective connectivity from the STN to the cortex, we studied the cortical evoked potentials via single pulse stimulation (constant current square wave, 0.3 ms, 1 Hz, 2 mA) of the STN. The technique was also described as cortico-cortical evoked potentials that was introduced to track the effective cortico-cortical connections in vivo in humans.[34,35] The test was also performed extra-operatively during the resting state. In the present study, the STN was stimulated through 2 adjacent contacts within the STN showing the most obvious propagated ictal discharges. Fifty stimuli were delivered. Simultaneous SEEG from unstimulated contacts were recorded. Cortico-cortical evoked potentials can, thus, be flexibly described as the STN-cortical potentials in the current study.

To evaluate the modulatory effects of STN stimulation and the potential varied cortical responses to distinct stimulation frequencies, a serial incremental stimulation frequency from 10 to 130 Hz, 90 ms pulse width, and intensity of 2 mA on the cycle pattern that lasted 60 seconds ("ON") with an interval of 60 seconds ("OFF") was applied on the STN. The contact within the STN, which also showed the most obvious propagated ictal discharges, was selected for cathodal referential stimulation with the adjacent one as an anode. Concurrent unstimulated contacts on distributed cortical areas were continuously recorded during the procedure.

Data Processing and Statistical Analysis

SEEG data were processed off-line using EEGLAB and customized MATLAB codes (MathWorks, Natick, MA) unless otherwise indicated. Bipolar montage from the adjacent contacts of each SEEG electrode was routinely used to highlight LFPs and reduce volume conduction. Moreover, LFPs were band-pass

filtered (butterworth bandpass, zero-phase shift) in the range of 0.5 to 250 Hz unless otherwise indicated. The SEEG data were initially screened by visual inspection, and the epochs with significant artifacts were discarded for further analysis. Because the voltage of LFPs inside the STN is weak, it was rescaled for visualization in comparison to cortical activity if necessary. For each patient, representative contacts of SEEG electrodes within the STN, seizure onset zone, early propagation areas, and other distributed cortical areas were manually selected. The locations of individual contacts were determined by anatomic landmarks visually.

With respect to the clinical seizures, ictal discharges were first reviewed. Ictal discharge pattern dependent analysis was thereby performed to probe the characteristics and propagation.[36] For tonic/clonic seizures, spectrograms of LFPs were carried out to display beta-gamma ictal discharges using continuous

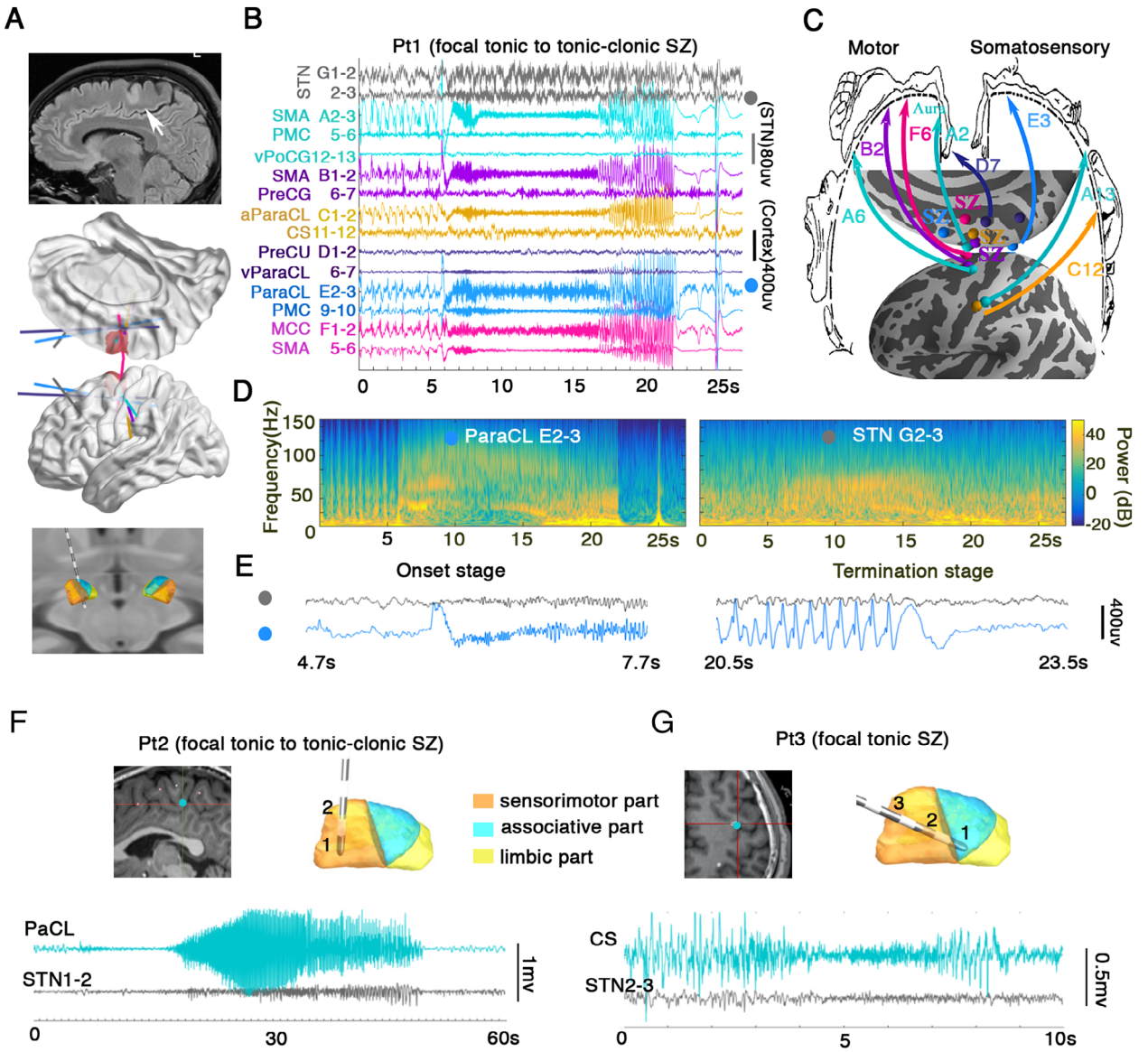


FIGURE 1: Propagation of motor seizures from motor strip to STN. (A–E) Patient 1. (A) Increased signal (arrow) on the left supplementary motor area (SMA, upper). The reconstructed all 7 stereoelectroencephalography (SEEG) electrodes overlaid on semitransparent cortical surface with red-coded the lesion (middle) and the SEEG electrode into the left STN (low). The color-coded electrodes were corresponded to the SEEG traces. (B) SEEG epoch of one asymmetric tonic seizure arising from the left SMA and paracentral lobule. Notably, fast amplitude ictal discharges propagated into the ipsilateral subthalamic nucleus (STN) almost simultaneously. (C) The results of electric cortical stimulation (ECS) of representative contacts were projected on Penfield's motor-somatosensory atlas. (D) Spectrogram of two traces on seizure onset zone (SOZ) and STN, respectively. (E) The zoom-in epoch highlighted the seizure propagation from SMA to STN during seizure onset and termination stages. The propagation of motor seizures to the ipsilateral STN in Patients 2 and 3 are shown in (F) and (G), respectively. STN = subthalamic nucleus; SMA = supplemental motor area; SOZ = seizure onset zone; SZ = seizure; PMC = ventral premotor cortex; vPoCG = ventral post central gyrus; PreCG = pre-central gyrus; aParaCL = anterior paracentral lobule; CS = central sulcus; PreCU = precuneus; vPaCL = ventral paracentral lobule; PMC = premotor cortex; MCC = middle cingulate cortex; ParaCL = paracentral lobule; INS = insula; ECS = electric cortical stimulation.

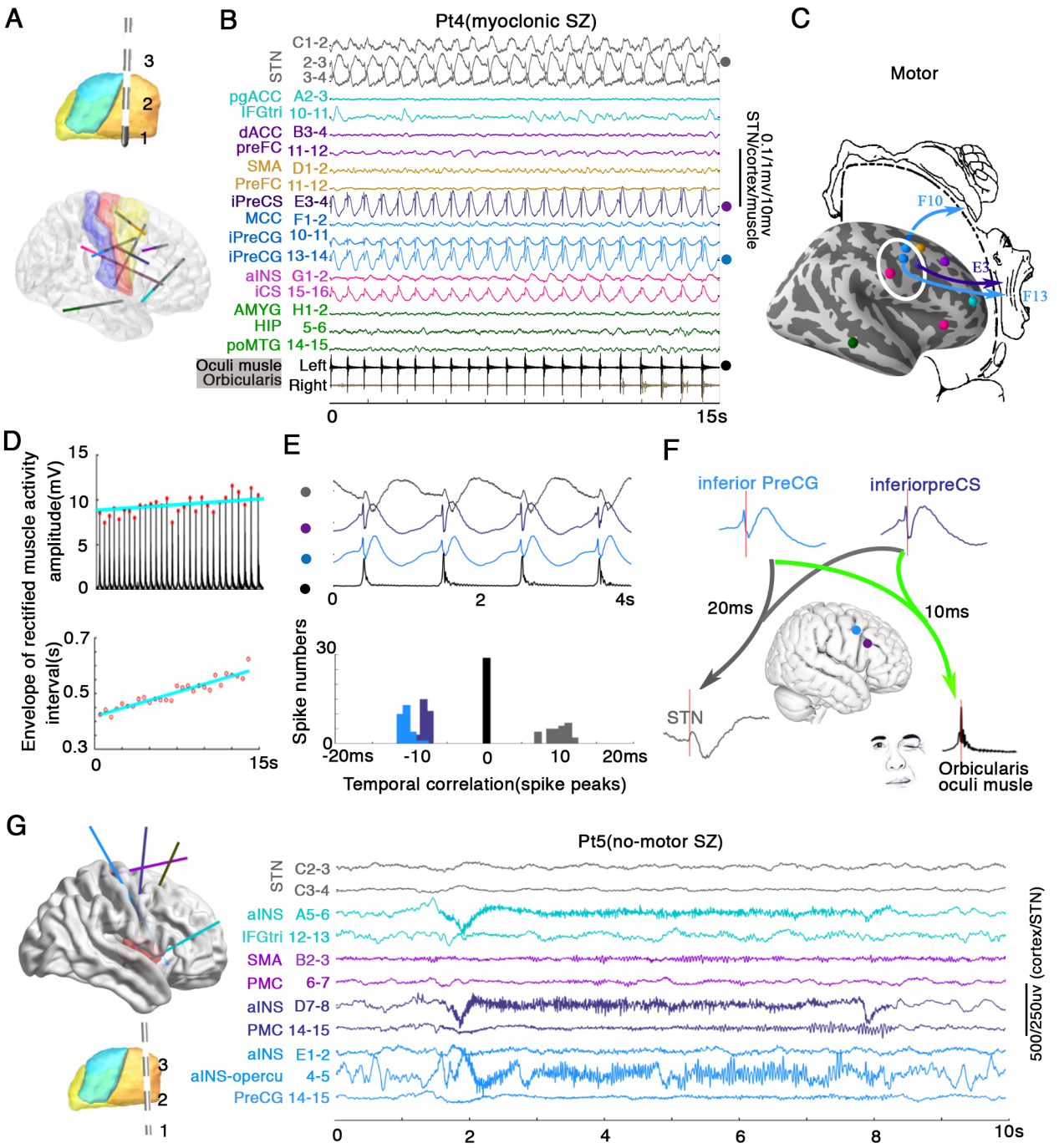


FIGURE 2: Propagation of myoclonic and nonmotor seizures. (A–F) Patient 4. (A) The stereoelectroencephalography (SEEG) electrode into the left subthalamic nucleus (STN; upper), and the reconstructed all 8 SEEG electrodes overlaid on semitransparent cortical surface (low). Blue, red, and yellow-coded strips indicate postcentral gyrus, precentral gyrus, and premotor cortex, respectively. (B) SEEG epoch of consecutive myoclonic jerks on the left side of the face. The rhythmic spike-waves on the right inferior precentral gyrus, inferior central sulcus, and premotor area were synchronized with STN and oculi muscle orbicularis activity. (C) Electric cortical stimulation results on Penfield's motor-somatosensory atlas. (D) The increment amplitude of rectified muscle activity (upper) and the gradually increased inter-jerk intervals (low) of the consecutive myoclonic jerks. (E) The zoom-in SEEG epoch (2 seconds) of representative traces in the seizure onset zone (SOZ), STN, and the envelope of rectified electromyography (EMG) of the oculi muscle orbicularis (upper), and histogram of the temporal correlation of cortical, ipsilateral STN spike peaks and muscle peaks (set to zero) by averaging consecutive 29 times spike peaks (low). (F) The schematic figure showed early (about 10 ms) and delayed (about 20 ms) propagation from motor cortex to muscle and to the STN. (G) Patient 5. (left) The SEEG electrode into the left STN and the reconstructed all 5 SEEG electrodes overlaid on semitransparent cortical surface (right). The corresponded SEEG epoch showed the STN was not affected by nonmotor seizure of ictal autonomic symptom arising from the insula. pgACC = pregenual anterior cingulate cortex; lFGtri = inferior frontal gyrus triangularis; dACC = dorsal anterior cingulate cortex; preFC = pre-frontal cortex; iPreCS = inferior precentral sulcus; aINS = anterior insula; iCS = inferior central sulcus; AMYG = amygdala; HIP = hippocampus; poMTG = post middle temporal gyrus.

wavelet transform. For myoclonic seizures, the periodic ictal discharges corresponded to the myoclonic jerks across representative areas were analyzed to further detect the precise propagation of temporal correlations from the cortex to the STN. In brief, the envelope of the rectified surface EMG was calculated. The peaks and inter-peak intervals of the consecutive burst muscle activity were detected to display the dynamics of rhythmic myoclonic jerks. The peaks of ictal discharges on representative contacts were also detected. For each myoclonic jerk, time zero was defined as the peak of burst muscle activity to compare the temporal relationship with the ictal spikes on distributed cortical sites and the STN.

The STN-cortical evoked potentials were averaged off-line and time locked to the onset of each electrical stimulus with a time window of −200 to 400 ms. The trials that were obviously contaminated with interictal discharges by visual inspection were discarded. In addition, considering signals were typically saturated and contaminated with stimulus artefacts from stimulus onset up to 10 ms, the first 10 ms epoch after stimulation was excluded from the analysis. To quantitatively reflect the connectivity strength from the STN to distributed cortical sites and how evoked responses compare with baseline, the t value between the 50 root mean square values of individual non-averaged post-stimulation epoch (10 to100 ms) and the 50 root mean square values of individual non-averaged pre-stimulation epoch (−200 to -10 ms) were measured using the paired two-sample *t*-test, which was validated in prior studies.[37,38] Positive significance ($t > 2$), not significance ($-2 < t < 2$) and negative significance ($t < -2$) CCEP t-values (corresponding to $p > 0.05$) was determined.

Regarding the modulatory effects of the STN stimulation, the classical epileptogenic biomarkers of interictal spikes (IIS) and high-frequency oscillations (HFOs) during stepwise increment stimulation were quantitatively calculated by automatic detection. For IIS, raw LFPs were first frequency band-pass filtered at 30 to 80 Hz and signal rectification, then the events above 3 SD on baseline were detected. Sequentially, the events that were above 10 SD of baseline and the interval was < 40 ms

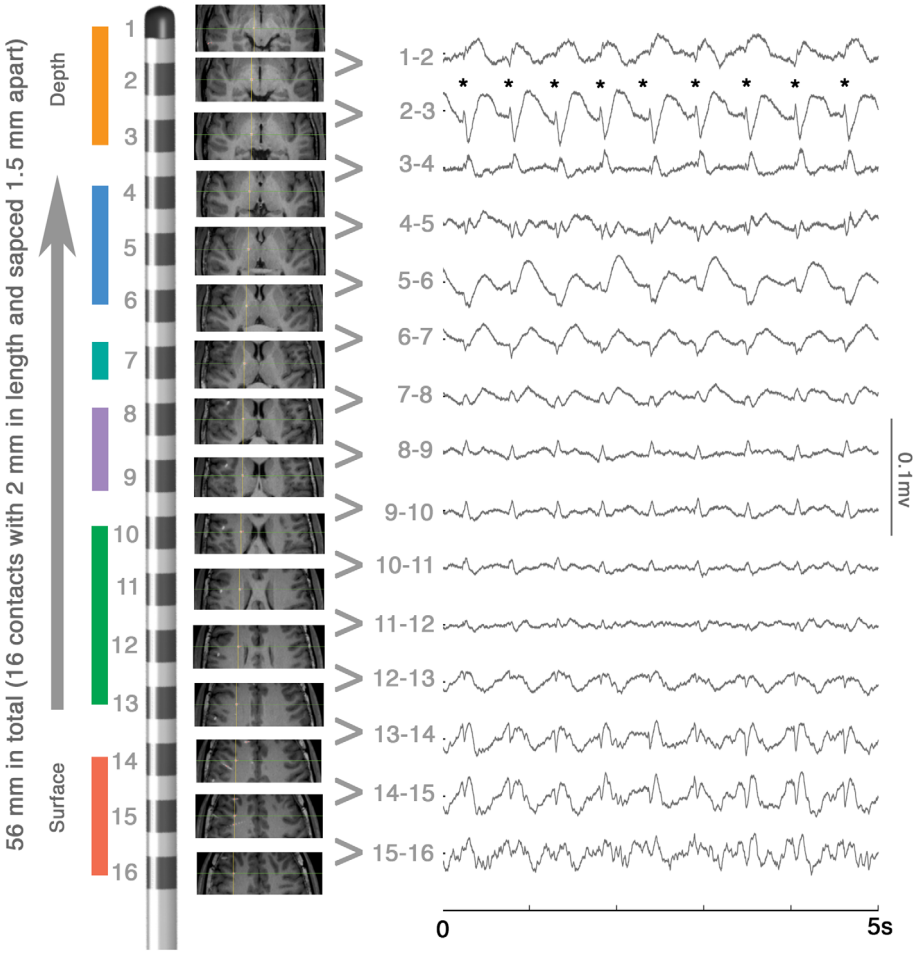


FIGURE 3: Stereoelectroencephalography (SEEG) traces along one electrode from the cortex to the subthalamic nucleus (STN). (Patient 4) It showed the ictal discharges during rhythmic myoclonic jerks on all consecutive contacts along one electrode that went through the bottom of the superior frontal sulcus, white matter, capsule, thalamus, and STN. Rhythmic spikes (black asterisk) could be visually detected on traces 2 to 3 that located into the STN. Of note, the neural activity was largely attenuated within the white matter. (The colors of orange-red, spring-green blue-violet, dark-cyan, steel-blue, and orange indicated the bottom of the superior frontal sulcus, white matter, capsule, thalamus, and STN.)

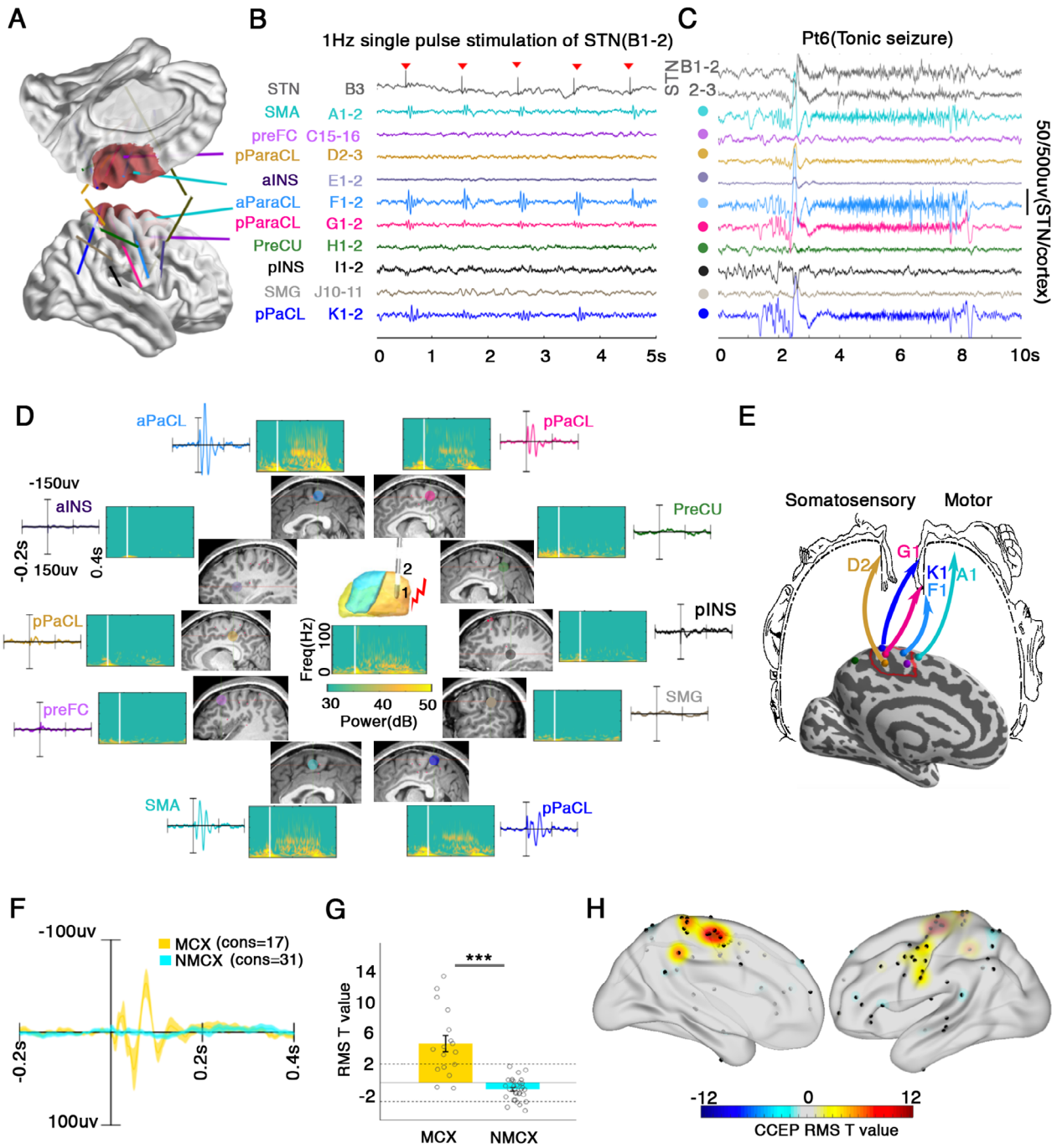


FIGURE 4: Cortical evoked responses to single pulse subthalamic nucleus (STN) stimulation. (A–E) Patient 6. (A) The reconstructed 11 stereoelectroencephalography (SEEG) electrodes on the cortex red-coded with the assumed seizure onset zone (SOZ; red-coded) mainly involving the paracentral lobule and the supplementary motor area (SMA). (B) The raw 5-second SEEG epoch during 1 Hz single pulse electric stimulation of the STN 1 to 2 (red triangles indicate the stimulation artifacts that was recorded on STN 3). The cortical responses can even be detected on motor areas visually. (C) One left leg tonic seizure arising from the right paracentral lobule and SMA with low amplitude beta-gamma ictal discharges. The traces on motor areas with initial ictal discharges were consistent with the ones with significate cortical responses to STN stimulation. (D) The paired display of the spectrogram of ictal discharges and averaged STN-cortical evoked potentials on representative contacts. The central images showed the reconstructed SEEG electrode into STN. (E) The results of ECS. (F–H) The STN-evoked cortical potentials at group level (n = 5). (F) STN-cortical evoked potentials on the motor and nonmotor cortex of representative contacts were averaged across patients (mean ± SEM), and (G) the comparison of RMS t value of cortical evoked potentials (10 to 100 ms after STN stimulation vs pre-stimulation −200 to -10 ms) between the motor and the nonmotor cortex using the paired t test (positive significance at $p < 0.05$: $t > 2$; negative significance at $p < 0.05$: $t < -2$), showing significant responses on the motor cortex than the nonmotor areas (***$p < 0.001$, rank sum test). (H) Spatial map of RMS t value of STN-evoked cortical potentials on Montreal Neurological Institute (MNI) standard template. The representative sites were accumulated of all 5 patients. For the purpose of demonstration, all the sites were collapsed onto the left side. pINS = post insula; SMG = supramarginal gyrus; RMS = root mean square; MCX = motor cortex; NMCX = nonmotor cortex.

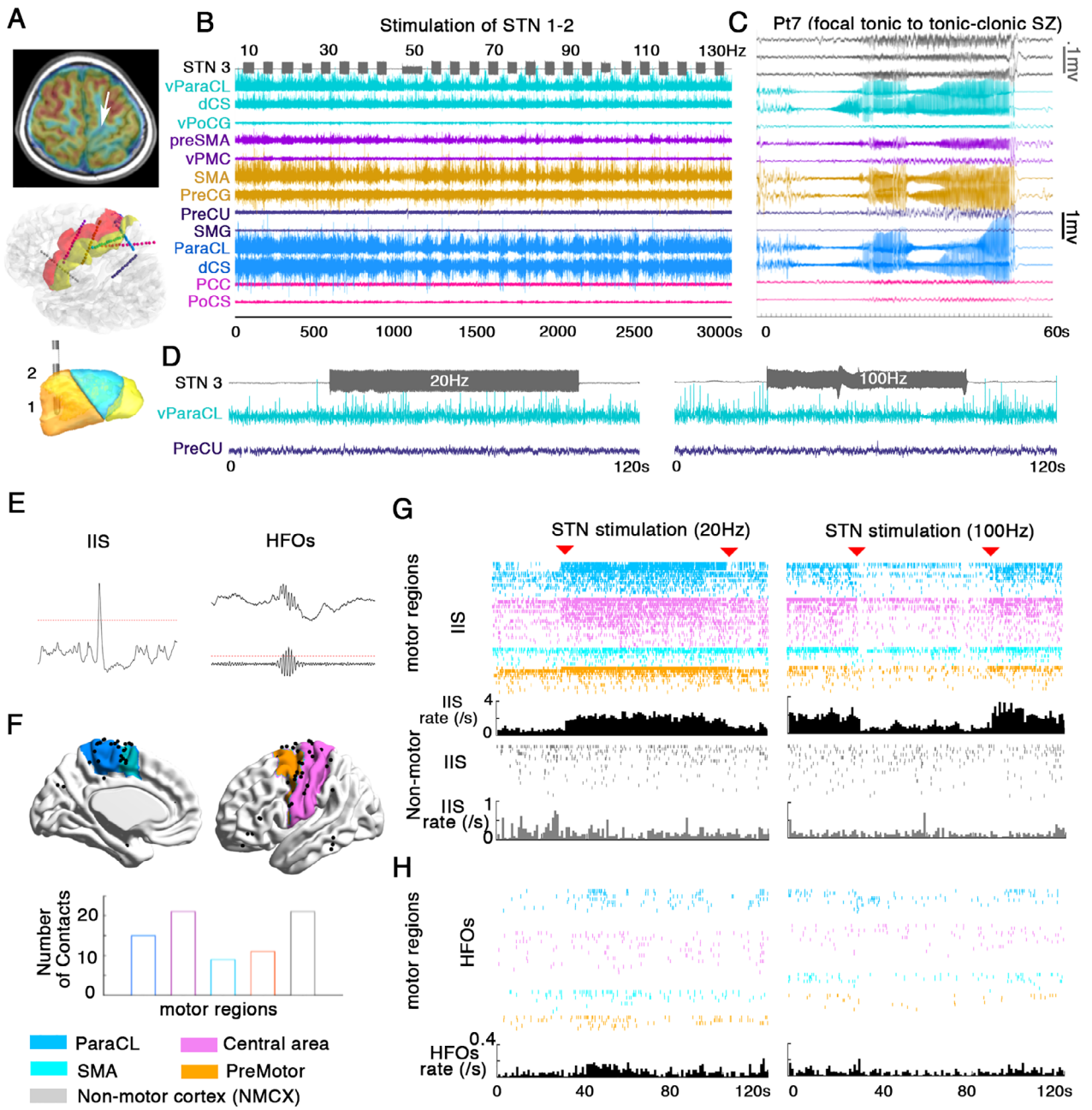


FIGURE 5: Cortical responses to subthalamic nucleus (STN) stimulation at stepwise increment frequencies. (A–D) Patient 7. (A) The hypometabolism mainly over the left upper and medial primary motor cortex on fluorodeoxyglucose-positron emission tomography (FDG-PET; arrow, upper). The reconstructed 7 stereoelectroencephalography (SEEG) electrodes overlaid on the cortical surface with red, yellow-coded precentral gyrus, postcentral gyrus (middle), and the SEEG electrode into the STN (low). (B) Highly compacted SEEG epoch showing simultaneous cortical responses when STN (1–2+) stimulation at stepwise increment frequencies from 10 to 130 Hz with "ON" (60 seconds) and "OFF" (60 seconds) cycle pattern. (C) SEEG epoch showed one right leg tonic seizure progressing into tonic-clonic seizure. Of note, the significant modulated traces in (B) were consistent with the ones inside the seizure onset zone (SOZ) over the motor cortex. (D) The zoom-in epochs of example cortical responses within SOZ on paracentral lobule and non-SOZ on precuneus at 20 Hz and 100 Hz, respectively. (E–H) At group level (n = 5), the impact of STN stimulation on interictal spikes (IIS) and high-frequency oscillations (HFOs; ripple) were quantitatively evaluated. (E) The example of automatic detected IIS and HFOs (above 3 STD from baseline). (F) The representative contacts from tested patients can be classified as distinct groups according to locations in standard Montreal Neurological Institute (MNI) space. (G) (upper) Raster plot showed IIS rates were remarkably increased when STN stimulation at 20 Hz over the motor areas but the nonmotor areas (low). In contrast, STN stimulation at 100 Hz produces reverse effect to decrease such epileptic activity on motor regions specifically (red triangles indicate the stimulation "ON" or "OFF"). (H) The same modulatory effect was also detected on HFOs rates over motor areas (pre-stimulation vs stimulation periods). Of note, the traces were ranked (vertical axis) of each region in increasing order according of their mean rate. dCS = dorsal central sulcus; PCC = posterior cingulate cortex; PoCS = post central sulcus; IIS = interictal spikes; HFOs = high-frequency oscillations; cons = contacts.

were eliminated. For HFOs, because the digital sampling at 4 to 5 times the oscillation frequency of interest is required to adequately reflect the temporal dynamics of HFO,[39] only HFOs at ripple band (100–250 Hz) were analyzed because only the sampling frequency of 1,024 Hz is available in our center currently. HFOs were identified using a previously described automated detection approach.[40] In brief, the criteria to detect the events, including at least 3 SD above the baseline and at least 4 consecutive peaks in the ripple frequency. To avoid the artifacts due to the filter, all detections were visually inspected for accuracy for each recording session. Next, the changes in the IIS and HFOs occurrence rates during 60 seconds of stimulation periods in comparison to the 30 seconds of prestimulation periods were also subsequently calculated. The reason that we chose 30 seconds rather than 60 seconds for the prestimulation period as baseline was to avoid the potential delayed modulatory effects of the previous stimulation as much as possible. Therefore, consecutive changes of cortical responses due to the stepwise stimulation frequency of the STN on distributed cortical areas were attained.

The Rank sum test was used to compare the cortical evoked potentials on the motor cortex and nonmotor cortex, as well as to compare the modulatory effects of the STN stimulation between the motor cortex and nonmotor cortex. The statistical significance level was set at $p < 0.05$.

Results

In total, 52 SEEG electrodes (7, 8, 6, 8, 5, 11, and 7 for Patients 1 to 7, respectively) with 744 contacts were implanted. There were no surgical-related complications in this group. The electrodes implanted into the brain were reconstructed for each patient. Electrodes that were designed to implant into the STN were mainly located at the sensorimotor part of the STN. The results from electric cortical stimulation showed that the seizure onset zones were mainly involving the motor cortex in all patients with the exception of Patient 5 who had seizures that arose from the anterior insular lobe.

Downstream Propagation of Ictal Discharges

Regardless of the various motor seizure semiology, we observed the consistent propagation of seizures from the motor cortex toward the STN across patients.

In Patient 1, an epileptic lesion that was assumed to be a focal cortical dysplasia was on the left supplementary motor area. Stereotypic asymmetrical focal tonic seizures on the right limb were recorded (Fig 1A–E). At the seizure onset, low amplitude fast activity at the beta-gamma band occurred from the left supplementary motor area and paracentral lobule. Remarkably, low amplitude fast activity appeared on the STN and synchronized with the cortical ictal discharges throughout the seizure almost simultaneously. The propagation pattern from the motor cortex to the STN was consistent in Patients 2, 3 (Fig 1F, G), 6, and 7. In Patient 4, stereotypic rhythmic, brachiofacial myoclonic jerks at approximately 1.5 to 2 Hz were recorded, which were time-locked to periodic ictal spikes over the lateral precentral gyrus, premotor area, and unilateral STN (Fig 2A–F). The consecutive rhythmic myoclonic jerks showed increased inter-jerk intervals and enhanced amplitude gradually. More precisely, it showed downstream propagation with stable temporal correlation of ictal spikes from motor cortex to the contralateral muscle about 10 ms and to the ipsilateral STN about 20 ms, respectively, suggesting the direct and indirect downstream propagation of motor seizures. Otherwise, the STN was

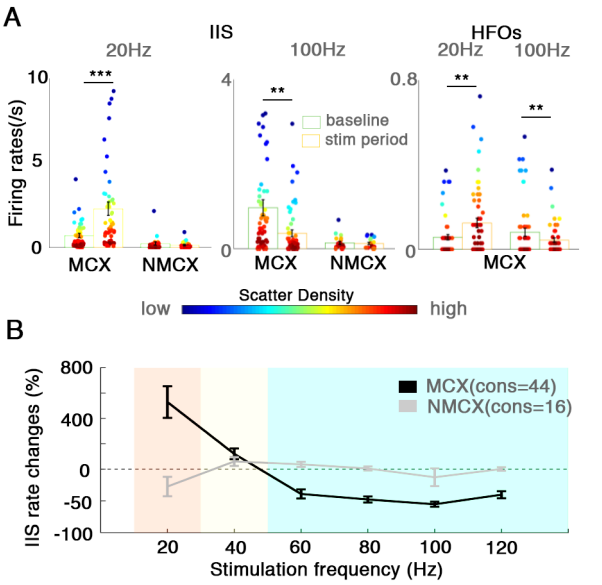


FIGURE 6: Location and frequency-dependent modulatory effect of subthalamic nucleus (STN) stimulation. (A) It showed the statistical significance of location-dependent (motor cortex vs nonmotor area) and frequency-dependent (representative low frequency at 20 Hz and high frequency at 100 Hz) modulatory effect on the interictal spikes (IIS) during the STN stimulation period compared with the prestimulation period. In addition, the high-frequency oscillation (HFO) rates were significantly modulated at 20 Hz (increased effect) and 100 Hz (decreased effect) during the STN stimulation period compared to the prestimulation period within the seizure onset zone (SOZ) that located on the motor cortex (*$p < 0.05$; **$p < 0.01$; ***$p < 0.001$, rank sum test). Of note, the individual firing rate of the IIS and HFOs was overlaid on bar in the manner of scatter density. (B) Using the changes of the IIS rates as biomarkers on the refined traces (the firing rate of IIS is more than 0.1/seconds), dynamic frequency and location dependent modulatory effect can be detected (mean ± SEM). Stimulation at high frequencies (> 50 Hz) that is semitransparent blue-shaded suggest therapeutic frequency window of STN-deep brain stimulation (DBS) in contrast to the deteriorating effect of low frequency (10–30 Hz) that is semitransparent pink-shaded. The semitransparent yellow-shaded frequency band (30–50 Hz) imply the frequency window with transitional effect.

unaffected during a nonmotor seizure that arose from the insular area in Patient 5 (Fig 2G).

To highlight the propagation of ictal discharges from the cortex to the STN, we demonstrated one example of SEEG traces on consecutive contacts along one electrode (Fig 3).

Cortical Evoked Responses to Single Pulse STN Stimulation

Cortical evoked responses to single pulse STN stimulation were examined in Patients 3, 4, 5, 6, and 7. Figure 4A–E showed one example of the time-locking evoked potentials to the electrical stimulation delivered through the SEEG electrode implanted into the STN in Patient 6. Clearly, the cortical potentials to single pulse stimulation of the STN were mainly detected within the seizure onset zone, which can be visually identified even in single pulse stimulation. The most robust responses, including the early component and late component, appeared with a latency of about within 100 ms after stimulation. The amplitude of the potentials showed marked variation among distributed cortical areas. However, the maximum amplitude occurred in the ipsilateral motor cortex, including the paracentral lobule and the lateral primary cortical strip as well as the supplementary motor area and premotor cortex.

At the group level (Fig 4F–H), the cortical evoked potentials on motor and nonmotor areas from the tested patients were averaged respectively for comparison. It also showed a significant difference of root mean square t value of cortical evoked potentials ranging from 10 ms to 100 ms compared with baseline between motor and nonmotor areas ($p < 0.001$). As indicated in the 3D display,

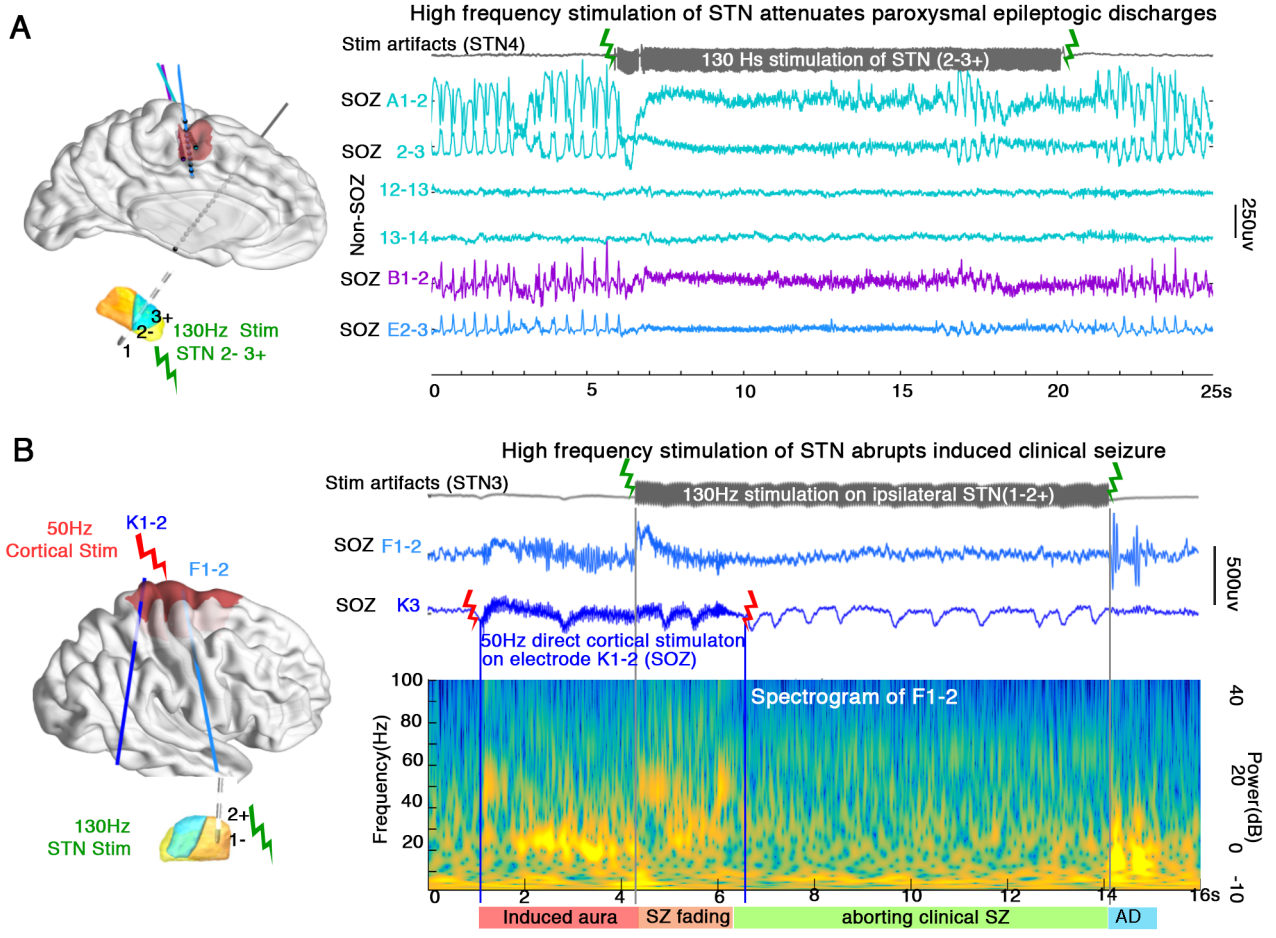


FIGURE 7: High-frequency stimulation of the subthalamic nucleus (STN) potentially attenuates subclinical and clinical motor seizures. (A) Patient 1. The reconstructed stereoelectroencephalography (SEEG) electrodes into the seizure onset zone (SOZ; red-coded) and the one that was implanted into STN. Only the electrodes that were tested were displayed. It showed high frequency stimulation at 130 Hz of the STN could dramatically attenuate the subclinical ongoing rhythmic epileptic discharges within the supplementary motor area (SMA), which sustained on the whole stimulation period. (B) Patient 6. An electric cortical stimulation (ECS; 50 Hz, lasting 5 seconds) of the contacts K 1 to 2 within the SOZ (red-coded) initially induced one aura of habitual tonic seizure. The evolving ictal discharges was interrupted almost simultaneously with the abortion of clinical seizure when high frequency stimulation at 130 Hz was instantly delivered on the STN. The recordings on adjacent contacts F 1 to 2 inside the SOZ showed the dynamic ictal discharges. AD = after discharge.

the spatial specificity of the cortical evoked responses to motor areas is remarkable.

Upstream Modulation of STN Stimulation on Epileptic Activity

Based on the map of reciprocal motor cortico-subthalamic circuit, we addressed the modulatory effects on motor seizures of STN stimulation at distinct stimulation frequencies. We observed the reproducible, prominent modulatory effects of the STN stimulation on the ipsilateral motor cortex specifically. Notably, the patients were unaware of the stimulation condition, and the natural movement was unaffected during stimulation.

Five patients (1, 4, 5, 6, and 7) underwent the stepwise increment stimulation procedure. An example result was demonstrated of Patient 7 (Fig 5A–D). The modulatory effect that varies among spatial distribution and are stimulation frequency dependent can be visually detected. The most modulated traces were responded to the ones within the seizure onset zone predominantly over motor cortex. At the group level (Fig 5E–H), the representative contacts from all tested patients were classified into 5 groups, including the paracentral lobule, lateral central gyrus, supplemental motor area, premotor area, and nonmotor area on the basis of the anatomic location. By quantitative analysis, STN stimulation at representative low frequency of 20 Hz increased IIS rates immediately within the motor areas compared with the nonmotor cortex. Conversely, STN stimulation at representative high frequency of 100 Hz produced a significant decreased IIS rates on motor areas. Because epileptogenic areas were mainly involving the motor cortex in this group, the detected HFOs were more spatially restricted in the motor areas. Thus, only the changes of HFO rates between prestimulation and stimulation periods were compared. In the motor cortex, HFO rates increased during 20 Hz STN stimulation compared to baseline but decreased when the STN was stimulated at 100 Hz. The statistical significance of the frequency and location-dependent modulatory effect is shown in Figure 6A. Moreover, dynamic frequency dependent modulatory effect was also detected (Fig 6B). STN stimulation below 30 Hz and above 50 Hz led to the dichotomically modulatory effect of increased or decreased epileptic activity on motor areas, suggesting the therapeutic frequency window of high-frequency stimulation in contrast to the deteriorating

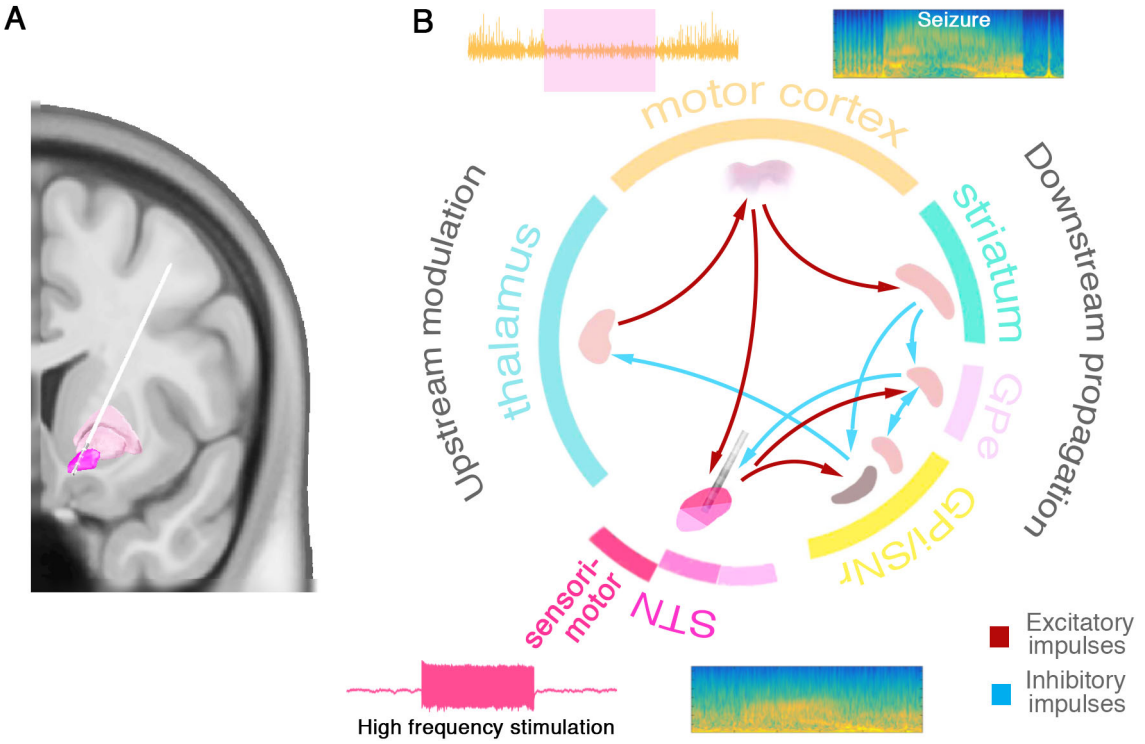


FIGURE 8: A model of the STN stimulation for modulating motor epileptic activity. (A) It showed the implantation of DBS lead into STN. (B) In the basal ganglia-thalamocortical loop, STN receive afferences from motor cortex directly (hyperdirect pathway) or through striatum and the external globus pallidus (indirect pathway) at the input level. In turn, STN send efferences to output structures of basal ganglia (GPi and SNr) or through external globus pallidus (GPe). GPi and SNr are connected to the ventral lateral nucleus of thalamo-cortical loop. Our data support STN is not only involved in as a propagation network of focal motor seizures but high-frequency stimulation of STN could specifically suppress the epileptic activity of the motor cortex via the basal ganglia-thalamocortical motor loop. (GPe = external globus pallidus; GPi = internal globus pallidus; SNr = substantia nigra pars reticulate).

effect of low frequency. Whereas frequencies from 30 to 50 Hz suggest the window of transitional modulatory effect.

In Patient 1 with frequently subclinical seizures, we had the chance to examine the effect of high-frequency stimulation of the STN on paroxysmal rhythmic discharges that were considered to be electrographic subclinical seizure patterns. It showed that STN stimulation at 130 Hz could attenuate ongoing rhythmic epileptic discharges on the motor cortex simultaneously. This effect lasted for the whole period of stimulation, and the activity quickly recovered within seconds after discontinuing the stimulation (Fig 7A). In Patient 6, it showed that STN stimulation at 130 Hz attenuated the evolving ictal discharges that arose from the motor cortex and potentially abort an ongoing clinical seizure that was successfully induced by electric cortical stimulation at 50 Hz (Fig 7B).

Finally, a model was conceived to characterize motor seizure downstream propagation toward the STN and upstream modulation of STN stimulation in the basal ganglia-thalamocortical network (Fig 8).

Discussion

Refractory seizures that arise from the motor cortex networks are associated with significant disability. They are organized in complex electrophysiological patterns that often involve both lateral and mesial aspects of premotor areas together with the precentral cortex.[41] To the best of our knowledge, our study, for the first time, provides the direct evidence in humans that the STN, the specific site within the interconnected cortico-subcortical network in sensory-motor integration and motor control, is not only engaged in as a propagation network of focal motor seizures but STN stimulation can profoundly modulate the epileptic activity of the motor cortex. Although we did not document the efficacy and safety in patients with epilepsy, we demonstrated a frequency-dependent upstream effect of simulating STN on the motor cortex specifically. High-frequency stimulation of the STN can reduce IIS and HFOs on the motor cortex and potentially attenuate the subclinical and ictal events, suggesting that the STN may be a preferable target of DBS for motor seizures.

STN-DBS has been extensively used in the clinical treatment of movement disorders and has been shown to be safe. The exploration of subcortical structures is a historical aspects of stereotactic exploration since its inception, particularly when stereotactic approaches were used to delineate tumors of the basal ganglia.[42] No complications related to the surgical procedure were reported in our patients and prior reports showed the safety of the thalamic exploration during SEEG.[43-45] The simultaneous recording of the thalamic nucleus and motor cortex enables investigation of its role in seizures and the effect of its stimulation at the individual level.

Our data clearly map the cortico-subthalamic loop in motor seizures by means of combined analysis of spontaneous seizure propagation and time-locked cortical evoked potentials to single pulse STN stimulation. In general, the application of STN-DBS in the treatment of Parkinson's disease has led to unprecedented understanding of the physiology and pathophysiology on the basal ganglia-cortex circuit. The STN plays a pivotal role in modulating the excitatory of the motor cortex via direct and indirect pathways. Although a similar subcortical pathway was observed during motor seizures in a primate model,[20] our data showed the prominent involvement of the STN in motor seizures propagation in humans. In turn, the effective connectivity from the STN to cortex has been previously showed by STN-DBS evoked scalp EEG potentials with the maximal amplitudes at the frontal midline and parasagittal scalp electrodes.[46] The direct cortical recordings of our data further evidence the effective connection of the STN to the motor cortex specifically. Thus, synchronous ictal discharges between the motor cortex and STN, together with the location-specific cortical evoked potentials to single pulse STN stimulation, delineate the reciprocal cortico-subthalamic circuit of motor seizures.

The distinct cortical-subthalamic circuit identified in our study is assumed to contribute to the specific upstream modulatory effects of STN stimulation on motor areas. Electrical stimulation can directly activate a wide range of neuronal elements in the STN and the surrounding area, including both afferent and efferent axons, producing not only orthodromic axonal activation but also an antidromic effect.[47] However, the exact mechanism of action of STN-DBS for modulating motor seizure activity is still to be clarified. The changes in IIS and HFO rates could be a reliable biomarker for treatment efficacy.[48,49] The significant reduction in IIS in conjunction with HFO rates on the motor cortex disclosing effective connections to the STN during the period of high-frequency stimulation suggests that the therapeutic role of STN-DBS for motor seizures. As our previous investigation of the effect of the anterior thalamic nucleus stimulation for the treatment of epilepsy,[44] high-frequency stimulation is assumed to desynchronize excessive cortical synchronization in epileptic condition via the motor cortico-subthalamic circuit at the level of LFPs, which might lower the pathological excitation of the motor cortex and reduce epileptic activity. In addition to the STN, the input structure of the globus pallidus externus within the cortico-basal ganglia circuit was also significantly affected by motor seizures in the primate model.[20] However, considering the profile of the small structure with little variability in localization,[50]

although other structures remain to be explored, it is reasonable to speculate that STN might be the preferred target for DBS.

Limitations of the present study include the small number of patients. Due to the invasiveness of intracranial recordings, incomplete cortical coverage, and less electrode sampling, the nonmotor cortex in our data is insufficient to evaluate the modulatory in each cortical area. In addition, considering the relative distinct subregions of the STN, only the modulatory effect of stimulating the sensorimotor part was studied in our study, the issue that whether stimulation of limbic or associative parts is effective to various epilepsy types is to be addressed. Finally, our preliminary observation that the attenuation of subclinical and clinical seizure by high-frequency stimulation STN-DBS warrants further investigation in larger numbers of patients, which holds the promise to develop closeloop responsive modulation for motor seizures.

Overall, STN-DBS has dramatically revolutionized the treatment of Parkinson's disease in regard to the improvement of motor symptoms dramatically over the past 20 years. Our data further supported the therapeutic modulation of STN-DBS for motor seizures, which would have significant implications for patients suffering from motor seizures when pharmacologic therapy fails.

Acknowledgments

Financial support

Liankun Ren was funded by the Beijing Natural Science Foundation (7202062) and the National Natural Science Foundation of China (81571271). Tao Yu was funded by the National Natural Science Foundation of China (81771395). Yuping Wang and Di Wang were funded by the National Natural Science Foundation of China (81771398). The authors would like to thank Cuiping Xu, Xiaohua Zhang, and Liang Qiao for the data acquisition, and Wei Du, Liping Li, Jialin Du, Runshi, Gao, Xiaoxia Zhou, Yanran Li, Di Wu, and Yuanyuan Piao for technical assistance. We would like to thank Professor Patrick Chauvel and Professor Gregory Worrell for critical discussion and reading of the manuscript. The authors are enormously indebted to the patients that participated in this study, as well as the nursing and physician staffs at each facility.

Author Contributions

L.K.R., T.Y., and Y.J.L. contributed to the conception and design of the study. L.K.R., T.Y., D.W., and XY.W. contributed to analysis of data. L.K.R., T.Y., D.W., G.J. Z, Y.P.W., F.B., and Y.J.L. contributed to drafting the text, preparing the figures, and interpreting the results. All authors reviewed and revised the manuscript for intellectual content.

Potential Conflicts of Interest

The authors declared no conflict of interest.

References

1. Gomez-Alonso J, Bellas-Lamas P. Surgical treatment for drug-resistant epilepsy. JAMA 2015;313:1572.
2. Vakharia VN, Duncan JS, Witt JA, et al. Getting the best outcomes from epilepsy surgery. Ann Neurol 2018;83:676–690.
3. Rosenow F, Luders H. Presurgical evaluation of epilepsy. Brain 2001; 124:1683–1700.
4. Jobst BC, Cascino GD. Resective epilepsy surgery for drug-resistant focal epilepsy: a review. JAMA 2015;313:285–293.
5. Heck CN, King-Stephens D, Massey AD, et al. Two-year seizure reduction in adults with medically intractable partial onset epilepsy treated with responsive neurostimulation: final results of the RNS system pivotal trial. Epilepsia 2014;55:432–441.
6. Morrell MJ, Group RNSSiES. Responsive cortical stimulation for the treatment of medically intractable partial epilepsy. Neurology 2011; 77:1295–1304.
7. Koubeissi MZ, Kahriman E, Syed TU, et al. Low-frequency electrical stimulation of a fiber tract in temporal lobe epilepsy. Ann Neurol 2013;74:223–231.
8. Fisher R, Salanova V, Witt T, et al. Electrical stimulation of the anterior nucleus of thalamus for treatment of refractory epilepsy. Epilepsia 2010;51:899–908.
9. Graber KD, Fisher RS. In: Noebels JL, Avoli M, Rogawski MA, et al., eds. *Deep brain stimulation for epilepsy: animal models*. Bethesda, MD: Jasper's Basic Mechanisms of the Epilepsies, 2012.
10. Zangiabadi N, Ladino LD, Sina F, et al. Deep brain stimulation and drug-resistant epilepsy: a review of the literature. Front Neurol 2019; 10:601.
11. Salanova V, Witt T, Worth R, et al. For the SANTE Study Group Long-term efficacy and safety of thalamic stimulation for drug-resistant partial epilepsy. Neurology 2015;84:1017–1025.
12. Cukiert A, Cukiert CM, Burattini JA, et al. Seizure outcome after hippocampal deep brain stimulation in patients with refractory temporal lobe epilepsy: a prospective, controlled, randomized, double-blind study. Epilepsia 2017;58:1728–1733.
13. Laxpati NG, Kasoff WS, Gross RE. Deep brain stimulation for the treatment of epilepsy: circuits, targets, and trials. Neurotherapeutics 2014;11:508–526.
14. Cukiert A, Lehtimaki K. Deep brain stimulation targeting in refractory epilepsy. Epilepsia 2017;58:80–84.
15. DeLong MR. Primate models of movement disorders of basal ganglia origin. Trends Neurosci 1990;13:281–285.
16. Okun MS. Deep-brain stimulation-entering the era of human neural-network modulation. N Engl J Med 2014;371:1369–1373.
17. Kato M, Malamut BL, Caveness WF, et al. Local cerebral glucose utilization in newborn and pubescent monkeys during focal motor seizures. Ann Neurol 1980;7:204–212. 30-2.
18. Caveness WF, Kato M, Malamut BL, et al. Propagation of focal motor seizures in the pubescent monkey. Ann Neurol 1980;7: 213–221. 32-5.

19. Kaniff TE, Chuman CM, Neafsey EJ. Substantia nigra single unit activity during penicillin-induced focal cortical epileptiform discharge in the rat. Brain Res Bull 1983;11:11–13.

20. Devergnas A, Piallat B, Prabhu S, et al. The subcortical hidden side of focal motor seizures: evidence from micro-recordings and local field potentials. Brain 2012;135:2263–2276.

21. Prabhu S, Chabardes S, Sherdil A, et al. Effect of subthalamic nucleus stimulation on penicillin induced focal motor seizures in primate. Brain Stimul 2015;8:177–184.

22. Benabid AL, Koudsie A, Benazzouz A, et al. Deep brain stimulation of the corpus luysi (subthalamic nucleus) and other targets in Parkinson's disease. Extension to new indications such as dystonia and epilepsy. J Neurol. 2001;248:37–47.

23. Chabardes S, Kahane P, Minotti L, et al. Deep brain stimulation in epilepsy with particular reference to the subthalamic nucleus. Epileptic Disord 2002;4:S83–S93.

24. Lee KJ, Jang KS, Shon YM. Chronic deep brain stimulation of subthalamic and anterior thalamic nuclei for controlling refractory partial epilepsy. Acta Neurochir Suppl 2006;99:87–91.

25. Handforth A, DeSalles AA, Krahl SE. Deep brain stimulation of the subthalamic nucleus as adjunct treatment for refractory epilepsy. Epilepsia 2006;47:1239–1241.

26. Shon YM, Lee KJ, Kim HJ, et al. Effect of chronic deep brain stimulation of the subthalamic nucleus for frontal lobe epilepsy: subtraction SPECT analysis. Stereotact Funct Neurosurg 2005;83:84–90.

27. Vesper J, Steinhoff B, Rona S, et al. Chronic high-frequency deep brain stimulation of the STN/SNr for progressive myoclonic epilepsy. Epilepsia 2007;48:1984–1989.

28. Wang X, Du J, Wang D, et al. Long-term outcome of unilateral deep brain stimulation of the subthalamic nucleus for a patient with drug-resistant focal myoclonic seizure. Ann Transl Med. 2020;8:1–5.

29. Cossu M, Cardinale F, Casaceli G, et al. Stereo-EEG-guided radiofrequency thermocoagulations. Epilepsia 2017;58:66–72.

30. Horn A, Neumann WJ, Degen K, et al. Toward an electrophysiological "sweet spot" for deep brain stimulation in the subthalamic nucleus. Hum Brain Mapp 2017;38:3377–3390.

31. Almeida L, Deeb W, Spears C, et al. Current practice and the future of deep brain stimulation therapy in Parkinson's disease. Semin Neurol 2017;37:205–214.

32. Horn A, Li N, Dembek TA, et al. Lead-DBS v2: towards a comprehensive pipeline for deep brain stimulation imaging. Neuroimage 2018;184:293–316.

33. Ewert S, Plettig P, Li N, et al. Toward defining deep brain stimulation targets in MNI space: a subcortical atlas based on multimodal MRI, histology and structural connectivity. Neuroimage 2018;170:271–282.

34. Matsumoto R, Nair DR, LaPresto E, et al. Functional connectivity in the human language system: a cortico-cortical evoked potential study. Brain 2004;127:2316–2330.

35. Buser P, Bancaud J. Unilateral connections between amygdala and hippocampus in man. A study of epileptic patients with depth electrodes. Electroencephalogr Clin Neurophysiol 1983;55:1–12.

36. Jirsa VK, Stacey WC, Quilichini PP, et al. On the nature of seizure dynamics. Brain 2014;137:2210–2230.

37. Enatsu R, Gonzalez-Martinez J, Bulacio J, et al. Connections of the limbic network: a corticocortical evoked potentials study. Cortex 2015;62:20–33.

38. Tousseyn S, Krishnan B, Wang ZI, et al. Connectivity in ictal single photon emission computed tomography perfusion: a cortico-cortical evoked potential study. Brain 2017;140:1872–1884.

39. Zijlmans M, Worrell GA, Dumpelmann M, et al. How to record high-frequency oscillations in epilepsy: a practical guideline. Epilepsia 2017;58:1305–1315.

40. Ren L, Kucewicz MT, Cimbalnik J, et al. Gamma oscillations precede interictal epileptiform spikes in the seizure onset zone. Neurology 2015;84:602–608.

41. Bonini F, McGonigal A, Trebuchon A, et al. Frontal lobe seizures: from clinical semiology to localization. Epilepsia 2014;55:264–277.

42. Bancaud J GS, Talairach J. E.E.G. et S.E.E.G. dans les tumeurs cérébrales et l'épilepsie Paris, France; 1973.

43. Guye M, Regis J, Tamura M, et al. The role of corticothalamic coupling in human temporal lobe epilepsy. Brain 2006;129:1917–1928.

44. Yu T, Wang X, Li Y, et al. High-frequency stimulation of anterior nucleus of thalamus desynchronizes epileptic network in humans. Brain 2018;141:2631–2643.

45. Filipescu C, Lagarde S, Lambert I, et al. The effect of medial pulvinar stimulation on temporal lobe seizures. Epilepsia 2019;60:e25–e30.

46. Baker KB, Montgomery EB Jr, Rezai AR, et al. Subthalamic nucleus deep brain stimulus evoked potentials: physiological and therapeutic implications. Mov disord 2002;17:969–983.

47. Li Q, Ke Y, Chan DC, et al. Therapeutic deep brain stimulation in parkinsonian rats directly influences motor cortex. Neuron 2012;76:1030–1041.

48. Lundstrom BN, Van Gompel J, Britton J, et al. Chronic subthreshold cortical stimulation to treat focal epilepsy. JAMA Neurol 2016;73:1370–1372.

49. Zijlmans M, Jiruska P, Zelmann R, et al. High-frequency oscillations as a new biomarker in epilepsy. Ann Neurol 2012;71:169–178.

50. Lee PS, Crammond DJ, Richardson RM. Deep brain stimulation of the subthalamic nucleus and Globus pallidus for Parkinson's disease. Prog Neurol Surg 2018;33:207–221.